ISSN 0016-7932, Geomagnetism and Aeronomy, 2021, Vol. 61, No. 6, pp. 810–818. © Pleiades Publishing, Ltd., 2021.
Russian Text © The Author(s), 2021, published in Geomagnetizm i Aeronomiya, 2021, Vol. 61, No. 6, pp. 713–722.

Radio Occultation Studies of Disturbances in the Earth's Ionosphere During a Magnetic Storm on June 22–23, 2015

V. N. Gubenko[a], *, V. E. Andreev[a], **, I. A. Kirillovich[a], *, T. V. Gubenko[a], ****, A. A. Pavelyev[a], *****, and D. V. Gubenko[a], ******

[a] *Kotel'nikov Institute of Radio Engineering and Electronics, Russian Academy of Sciences, Fryazino, Moscow oblast, 141190 Russia*

**e-mail: gubenko@fireras.su, vngubenko@gmail.com*

***e-mail: v.e.andreev@gmail.com*

****e-mail: sabersecretmail@gmail.com*

*****e-mail: chif1989@gmail.com*

******e-mail: alxndr38@gmail.com*

*******e-mail: mar4ello19922@gmail.com*

Received February 27, 2021; revised April 17, 2021; accepted May 27, 2021

Abstract—The results of ~100 sessions of sounding of the Earth's high-latitude (>65° N) ionosphere performed on June 22–23, 2015, at a GPS carrier frequency of f_1 = 1575.42 MHz ($L1$ range, wavelength of ~19.0 cm) in the FORMOSAT-3/COSMIC radio occultation experiment are analyzed. The coronal plasma ejections that reached the Earth's magnetosphere during this time period provoked a strong magnetic storm of the $G4$ class ($G4 = Kp - 4$), which caused significant fluctuations in radio wave parameters on ionospheric sounding paths: navigation (GPS) satellites—low-orbit (FORMOSAT-3/COSMIC) satellites. Ionospheric disturbances in the characteristics of radio waves are shown to be caused by both geomagnetic conditions and the activity of powerful X-ray flares during measurements. A search for the absorption of decimeter radio waves (wavelength of ~19 cm) at a GPS carrier frequency of f_1 = 1545.42 MHz was carried out. Based on the results of the FORMOSAT-3/COSMIC data analysis, an integral absorption of ~3 dB of decimeter radio waves was detected for the first time on the sounding paths in the D and E regions of the Earth's high-latitude ionosphere.

DOI: 10.1134/S0016793221060050

1. INTRODUCTION

In June 2015, coronal mass ejections (CMEs) towards the Earth (one main and several small ejections) occurred on the Sun. This event was recorded by spacecraft (three satellites Swarm A, B, and C; ACE (Advanced Composition Explorer) spacecraft), and ionospheric stations (Reiff et al., 2016; Baker et al., 2016; Astafyeva et al., 2016, 2017; Mansilla, 2018; Yasyukevich et al., 2020). The approach of the main CME to the Earth's magnetosphere and its interaction with the shock wave was expected at ~1836 UT on June 22, 2015, after a weaker shock at ~0540 UT (Reiff et al., 2016). This event was accompanied by strong changes in the proton density and the solar-wind velocity, as well as the (Bx, By, Bz) components of the interplanetary magnetic field (IMF) (Astafyeva et al., 2017). The magnetometer of the ACE spacecraft recorded the most powerful solar plasma ejection as an IMF jump from ~10 to ~40 nT. The Solar Wind Electron, Proton, and Alpha Monitor (SWEPAM) instrument detected this outburst by registering a sudden increase in proton density from ~20 to ~45 particles/cm^3 with a corresponding increase in the solar-wind pressure to values greater than 50 nPa (Reiff et al., 2016). Reiff et al. (2016, Fig. 1) give in detail the geomagnetic conditions during the storm (proton density, solar-wind velocity and pressure; the Bx, By, Bz components, and the angle of the IMF vector) on June 22–23, 2015. The Boyle index, which is associated with the southward IMF component, sent a "yellow alarm" (Kp index greater than 4) on June 22 at 0604 UT and a "red alarm" (Kp index equal to 6 or greater) on June 22 at 1834 UT, just before the collision of the main plasma ejection with the shock wave (Reiff et al., 2016, Fig. 1d). Astafyeva et al. (2016) analyzed variations in the electron density (N_e) and the vertical total electron content (TEC) for the upper part of the ionosphere at altitudes of ~460 km (Swarm A and C) and ~530 km (Swarm B) in the initial and main phases of the magnetic storm on June 22–23, 2015, based on data from the Swarm A, B, and C satellites. A significant daytime increase in the vertical TEC and N_e was detected at all latitudes in the initial phase of the storm (~19–

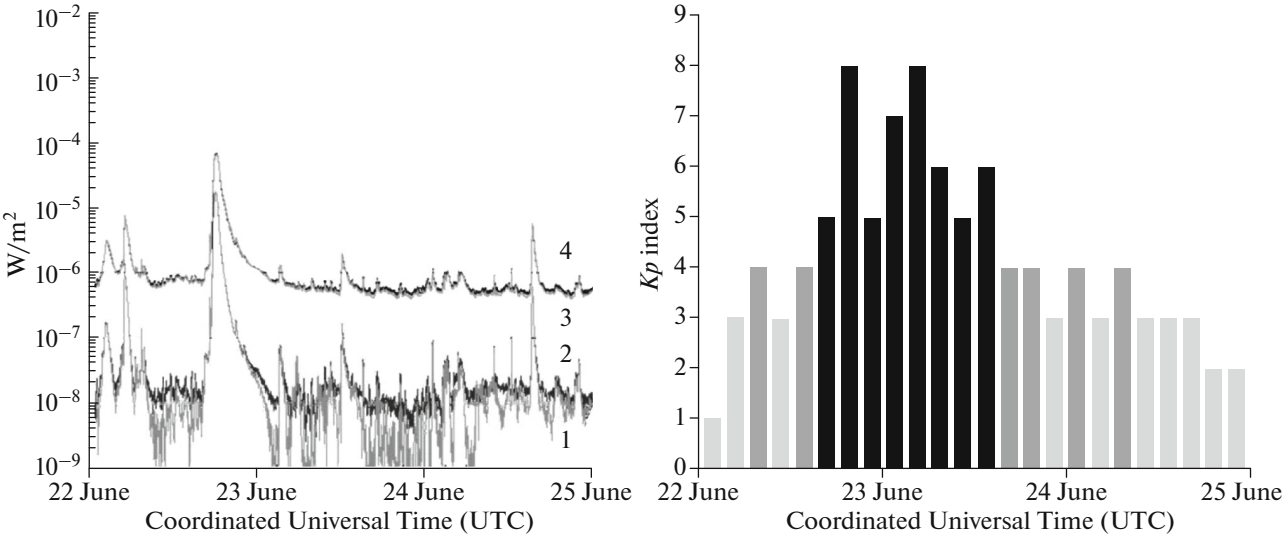

Fig. 1. X-ray fluxes (1-min data, left panel) recorded by the GOES-13 and GOES-15 geostationary spacecraft in the ranges of 0.05–0.40 nm (1, GOES-15; 2, GOES -13) and 0.10–0.80 nm (3, GOES-15; 4, GOES-13) on June 22–23, 2015. Planetary *Kp* index values (3-h data, right panel) (URL: ftp://ftp.swpc.noaa.gov/pub/warehouse/).

21 UT on June 22) and at the end of the main phase of the storm (~03–05 UT on June 23).

The arrival of the main CME at the Earth's magnetosphere on June 22 at ~1836 UT practically coincided in time with powerful bursts of X-ray radiation (~1800 UT is the time of maximal X-ray fluxes), which were recorded by the geostationary satellites GOES-13 and -15 (Fig. 1, left panel). Figure 1 shows that the maximal flux values in the ranges of 0.05–0.40 and 0.10–0.80 nm exceed their background values by ~3 and ~2 orders of magnitude, respectively. The right panel of Fig. 1 shows the values of the planetary *Kp* index, which characterizes the geomagnetic conditions during the storm on June 22–23, 2015. These values were taken from the space weather data archive (URL: ftp://ftp.swpc.noaa.gov/pub/warehouse/).

Radio sounding of the Earth's atmosphere and ionosphere with aid of satellite-to-satellite communication lines by using the high-orbit (GPS/GLONASS) and low-orbit satellites was previously carried out in various combinations, e.g., GPS-MICROLAB, GPS-GRACE, GPS/GLONASS-METOP, GPS-CHAMP, GPS-FORMOSAT-3/COSMIC, and others. The experimental results have been analyzed in detail (Yakovlev et al., 2014; Gorbunov, 2017; Yakovlev et al., 2019). For the global study of the Earth's atmosphere and ionosphere in radio occultation experiments of the FORMOSAT-3/COSMIC mission, signals from GPS navigation satellites located in orbits with an altitude of ~20200 km above the Earth's surface are used. The receivers installed on six small FORMOSAT-3/COSMIC satellites (their orbital altitude is ~800 km) record the eikonal (phase path) and radio wave power at two GPS carrier frequencies of $f_1 = 1575.42$ MHz ($L1$ band, wavelength of ~19.0 cm) and $f_2 = 1227.6$ MHz ($L2$ band, wavelength of ~24.4 cm) as a function of time. The vertical velocity of the perigee of the radio ray when the FORMOSAT-3/COSMIC satellites are behind the planet is ~2 km/s. This value is many times higher than the characteristic velocities of the layers in the Earth's ionosphere and atmosphere. Since the typical duration of a radio occultation session is about 2 min, the satellite radio hologram contains an almost instantaneous image of the environment state in the studied area. With the known ballistic data of satellites and analysis of the changes in the eikonal (or phase) of the signal, it is possible to determine the impact parameter of the ray trajectory and the refraction angle of the radio ray. Next, various methods based on the Abel transform are used to determine the vertical profiles of the electron density in the ionosphere and the refractive index in the neutral atmosphere of the Earth (Liou et al., 2007). This is the traditional method for the reconstruction of the characteristics of the probed medium. It uses the geometrical optics (GO) approximation without allowance for diffraction effects. In GO, the vertical resolution is determined by the minimum vertical distance at which the Fresnel volumes of two physical rays do not intersect with each other and become distinguishable. Thus, the vertical resolution of the GO method corresponds to the size (diameter $d_f = 2r_f$) of the first Fresnel zone $d_f = 2r_f = 2(\lambda D)^{1/2} \sim$ 1.5 km, where $\lambda \sim 20$ cm is the wavelength of the sounding signal and $D \sim 3090$ km is the distance from the FORMOSAT-3/COSMIC satellite to the planet's atmospheric limb. When calculating the D value, we took into account that the average radius of the Earth is ~6370 km, and the height of the perigee of the radio ray in the ionosphere is ~100 km.

Studies of small-scale structures at high latitudes of the Earth's ionosphere are of great practical interest for radio communication and navigation, and they are also important for the analysis of the space weather dynamics. Sporadic *E* layers are known to be very thin, dense layers of increased ionization in the Earth's ionosphere at altitudes from ~90 to ~120 km. The theory of the formation of sporadic *E* layers at middle latitudes by means of wind shear has been confirmed in many studies. The wind-shear mechanism is less effective at high latitudes of planet than at the middle latitudes, because here the magnetic field is directed almost vertically to the local horizon. Therefore, the horizontal structure of plasma in the *E* and *D* regions of the aurora is determined by the spatial distribution of solar sources of particle precipitation (Gubenko et al., 2018).

We used radio occultation measurements to study sporadic *E* layers in the Earth's ionosphere. The parameters of the ionospheric layers were determined via analysis of the vertical profiles of the eikonal variations and the received signal intensity. This made it possible to estimate the spatial displacement of sporadic *E* structures relative to the perigee of the ray trajectory, to determine the inclination angles of the layers relative to the local horizon, and to find the actual heights of the layers (Pavelyev et al., 2012, 2015). Using inclined sporadic *E* layers as a detector, we developed a new method to reconstruct the characteristics of small-scale internal waves in the planet's ionosphere (Gubenko et al., 2018; Gubenko and Kirillovich, 2019, 2020). This method is based on the fact that an internal wave propagating through an initially horizontal sporadic *E* layer leads to turning of its ionization plane parallel to the wave phase front. The developed method makes it possible to study the relations between internal waves and sporadic *E* structures in the ionosphere and it also significantly expands the capabilities of traditional radio occultation monitoring of the Earth's atmosphere and ionosphere (Gubenko et al., 2018; Gubenko and Kirillovich, 2019, 2020).

Research of the absorption effects of radio waves in the Earth's ionosphere is very important to ensure the uninterrupted operation of radio communication and navigation systems. The potential ability to determine the absorption in the atmosphere and ionosphere of the planet was discussed earlier (Liou et al., 2007; Pavelyev et al., 2009, 2015; Wickert et al., 2004). Using analysis of altitude variations in the amplitude and phase of the radio occultation signal (*L*1 range, wavelength of ~19.0 cm), Pavelyev et al. (2015) found integral absorption from ~1 to ~4 dB of decimeter radio waves below ~15 km in the Earth's troposphere. However, at present, there are no radio occultation data on the absorption of decimeter radio waves at carrier GPS frequencies (wavelengths of ~19.0 and ~24.4 cm) in the Earth's ionosphere.

In this paper, we analyze the radio occultation measurements of the eikonal and power of signals received by the FORMOSAT-3/COSMIC satellites in order to search for the absorption of decimeter radio waves (*L*1 range, wavelength of ~19 cm) in the Earth's high-latitude ionosphere during a magnetic storm in June 2015.

2. SELECTION OF SESSIONS OF THE FORMOSAT-3/COSMIC SATELLITE MISSION AND ANALYSIS OF EXPERIMENTAL DATA

In this study, the results of processing (Level 1b and 2) of the FORMOSAT-3/COSMIC mission radio occultation measurements obtained at the Taiwan data center (http://tacc.cwb.gov.tw) are used as the initial information for the analysis. To solve this problem, ~100 sessions of radio occultation measurements on June 22–23, 2015, were selected from the large FORMOSAT-3/COSMIC database. The selected measurement sessions were performed at latitudes of ~65°–88° N and covered an altitude interval of ~50–110 km. Each of the analyzed sessions contained the dependences of the eikonal and signal power (*L*1 range) on the ray perigee altitude (Level 1b) and also had a vertical electron density profile (Level 2). The accuracy of the reconstruction of the electron density is of $\sim 10^4$ cm^{-3}, and its values are given with a vertical step of 2.5 km (an estimate of the vertical resolution). A measurement sampling rate of 50 Hz corresponds to a time resolution of 0.02 s for eikonal and signal power data. The processing of these measurements included smoothing of the experimental data over 15 points with the moving average method. With a sampling rate of 50 Hz and a vertical ray velocity of ~2 km/s, we find that the data smoothing interval is of ~0.6 km. Since this value is significantly less than the vertical resolution (~1.5 km) of the GO method, the data after smoothing retaine all information about the vertical small-scale structure in the Earth's ionosphere.

The goal of this work is to study disturbances in the *E* and *D* regions of the Earth's high-latitude ionosphere during a strong geomagnetic storm based on FORMOSAT-3/COSMIC radio occultation measurements from June 22 to June 23, 2015. With allowance for the effect of geomagnetic conditions and X-ray fluxes on the ionosphere, this period can be divided into three time intervals. The first interval starting on June 22 at 0000 UT and ending at 1630 UT of the same day is a quiet geomagnetic period, the end of which precedes the onset (~1630 UT, Fig. 1) of powerful X-ray bursts and the arrival (~1836 UT) of the main CME at the Earth's magnetosphere. This quiet period is characterized by low background values of X-ray fluxes and low geomagnetic activity with minimal changes in the IMF characteristics (Reiff et al., 2016). The second time interval (beginning June 22 at 1630 UT and ending June 23 at 0200 UT) is a period of powerful ionospheric disturbances caused by both the main phase of the magnetic storm and powerful bursts of X-ray

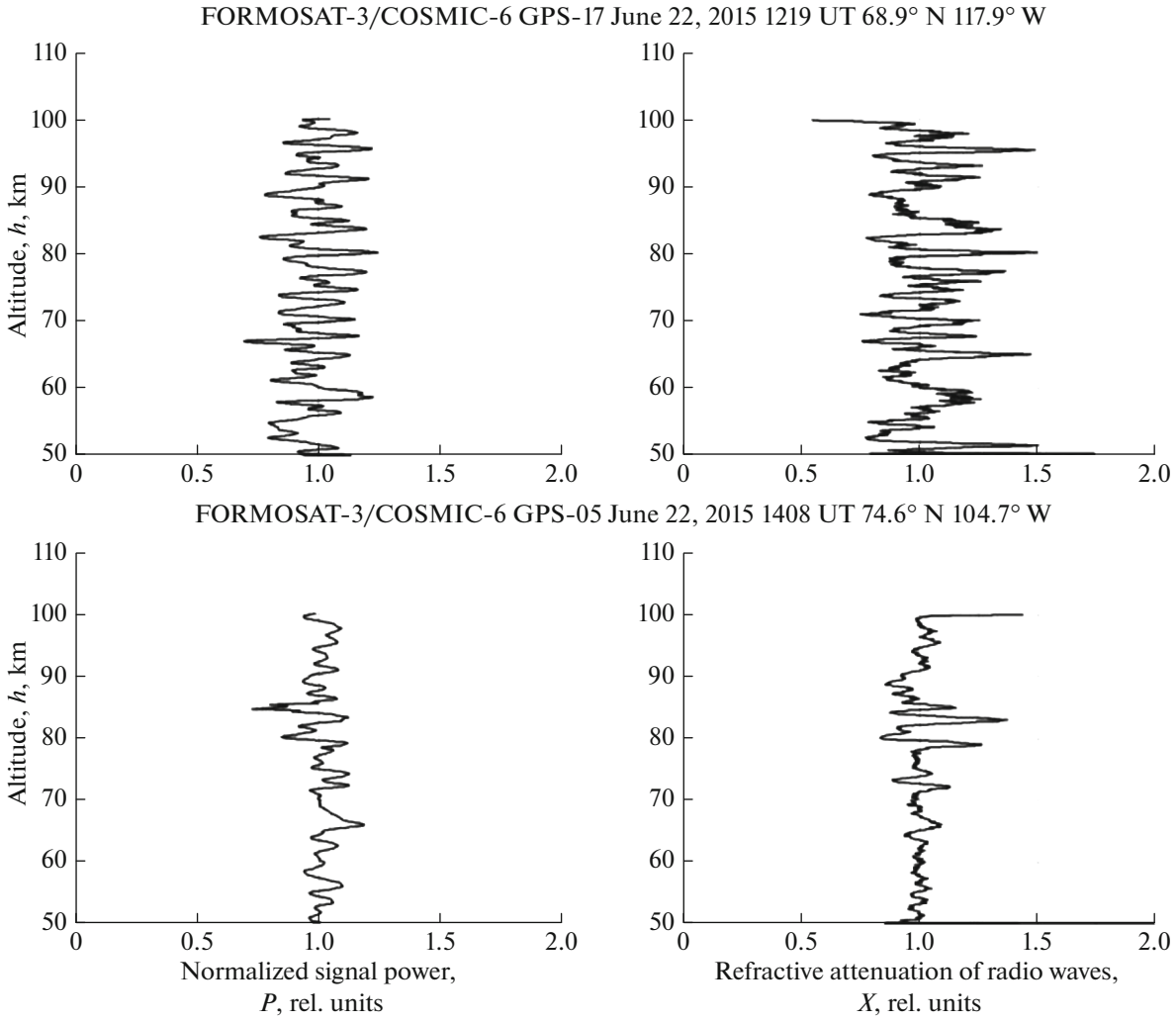

Fig. 2. Altitude profiles of the normalized signal power (P) measured by the FORMOSAT-3/COSMIC-6 satellite on the eve of the main phase of the magnetic storm on June 22, 2015, and the refractive attenuation profiles (X) reconstructed from the eikonal data.

fluxes. The third time interval (from 0200 UT to 2400 UT on June 23) is characterized by insignificant fluctuations of the eikonal and signal power during sounding sessions of the Earth's ionosphere. The beginning of this interval coincides in time with the end of powerful X-ray bursts (Fig. 1, left panel). Here, we observe a sharp decrease in proton density to ~5–10 cm^{-3} with a corresponding decrease in pressure to ~5–10 nPa (Reiff et al., 2016; Astafyeva et al., 2017). Starting from this moment in time, the IMF Bz component sharply decreases to –27 nT and remains negative until ~0530 UT on June 23 (Astafyeva et al., 2017). The analysis shows that the third time interval is a quiet period without intense fluctuations of radio waves during ionospheric sounding, although the values of the planetary Kp index during this period were notable (Fig. 1, right panel). It should be noted that a significant number of the sessions selected for analysis were performed within the first and third time intervals. The perturbations of the vertical profiles of the normalized signal power on sounding paths in the E and D regions in the Earth's ionosphere are insignificant for these measurement sessions. Typical examples will be considered below in Fig. 2.

Studies (Yakovlev et al., 2014; Gubenko et al., 2018; Gubenko and Kirillovich, 2019) have shown that there is a relationship between the power (P_L) of the radio occultation signal received on a LEO satellite, the refractive attenuation of radio waves (X), and the acceleration (a_ψ) of the eikonal (phase path ψ):

$$1 - X(t) = ma_\psi = md^2\psi/dt^2, \quad m = r_\psi/(dp_0/dt)^2, \quad r_\psi = L_L L_G/L_0, \tag{1}$$

where p_0 is the impact parameter of the radio ray, L_L and L_G are the distances from the receiver (L) and

transmitter (G) to the ray perigee point, respectively, and L_0 is the distance from the transmitter to the receiver along a straight line (Yakovlev et al., 2014). Figure 2 shows typical altitude profiles of the normalized signal power (P) measured by the FORMOSAT-3/COSMIC-6 satellite before the main phase of the geomagnetic storm on June 22, 2015 and the refractive attenuation profiles (X) reconstructed from signal eikonal data with the use of expressions (1). The analyzed sessions of radio occultation measurements in the Earth's ionosphere were performed on June 22, 2015, at 1219 UT (upper panel) and 1408 UT (lower panel) in a quiet geomagnetic period (first time interval), on the eve of powerful X-ray bursts and before arrival of the main CME at the planet's magnetosphere. The curves in Fig. 2 were obtained via smoothing of the experimental data over 15 points with the moving-average method. As discussed above, the data smoothing interval is ~0.6 km, although the vertical resolution of the GO method is ~1.5 km. To find the P dimensionless value, the P_L power of the signal received on the FORMOSAT-3/COSMIC-6 satellite was normalized to the average value of the power (P_0) of radio waves at altitudes over 300 km, i.e., $P = P_L/P_0$. The numbers of low-orbit (FORMOSAT-3/COSMIC) and navigation (GPS) satellites, the date and time of the measurement session, and the coordinates (latitude and longitude) of the sounded area are shown above each part of Fig. 2. To estimate the fluctuation levels in the analyzed power profiles $P(h)$, we used the S4-index, which is defined as the standard deviation normalized to the average signal power (Yasyukevich et al., 2020). The values of the S4-index for profiles $P(h)$ analyzed in Fig. 2 were found to be ~18% (top panel) and ~10% (bottom panel). The analysis showed that the profiles of power $P(h)$ and refractive attenuation $X(h)$ for sessions of the first interval (quiet geomagnetic period) demonstrate weak disturbances in the E and D regions (50–100 km) of the Earth's high-latitude ionosphere. Thus, the S4-index values did not exceed ~20% for all power profiles $P(h)$, which were obtained from radio occultation measurements performed within the first time interval.

Based on the analysis of radio occultation data, it is difficult to determine the beginning of a magnetic storm. It should be noted that fluctuations in the power $P(h)$ and refractive attenuation $X(h)$ of the radio occultation signal increase strongly starting with the beginning of powerful bursts (~1630 UT on June 22, Fig. 1) of X-ray radiation in the Earth's ionosphere. It is known that a powerful and sharp burst of X-ray flux can be a time stamp for the study of solar flares (Hocke, 2008). The GOES-13 and GOES-15 satellites, which are located in geostationary orbits, continuously measure solar X-ray fluxes in two wavelength ranges: the first range is from 0.05 to 0.40 nm, and the second range from 0.10 to 0.80 nm. Figure 1 shows that a sharp increase in X-ray fluxes (~1000 times for the range from 0.05 to 0.40 nm, and ~100 times for the range from 0.10 to 0.80 nm) occurs on June 22 during a short time interval of 1630–1800 UT. The moment of the X-ray burst at ~1800 UT on June 22 is clearly determined by the time of the maximum of the X-ray flux. The data analysis shows that the N_e electron density in the Earth's ionosphere increases to values of $\sim 10^5$ cm^{-3} or higher for those radio occultation sessions in which the measurement time practically coincides with the time of the most powerful X-ray burst (~1800 UT, Figs. 1, 3, and 4).

The two vertical profiles shown in Fig. 3, $P(h)$ and $X(h)$, were obtained from radio occultation measurements performed on June 22 at 1730 UT (left, second time interval) and on June 23 at 0203 UT (right, third interval) in the Earth's high-latitude ionosphere. Measurements related to the profiles on the left side of Fig. 3, were performed ~1 h after the beginning (~1630 UT) of powerful X-ray bursts and ~1 h before the arrival (~1836 UT) of the main CME at the planet's magnetosphere. These measurements are affected only by X-ray bursts; they are not affected by the geomagnetic conditions of the main storm phase. The S4-index value for the analyzed $P(h)$ variations shown in Fig. 3 (left, panel a) was found to be ~28% at heights (~80–100 km) of the transition zone from the E to D region of the Earth's high-latitude ionosphere.

An isolated sporadic E layer with a vertical size of ~2.0 km was observed at a ray perigee altitude of ~93.7 km (Fig. 3, left, panel a). It has a typical U-shape, which was previously reported in (Zeng and Sokolovskiy, 2010), with oscillations (wave optics effects) above and below the defocusing region caused by the interference of the direct and refracted rays at the layer boundaries. As can be seen, the results of reconstruction of the refractive attenuation $X(h)$ by the GO method (Fig. 3, left, panel b) are in good agreement with the power $P(h)$ values, but without oscillations at the layer boundaries. Computer-simulation data (Zeng and Sokolovskiy, 2010) and radio occultation studies (Gubenko et al., 2018; Gubenko and Kirillovich, 2019, 2020; Pavelyev et al., 2012, 2015) show that the altitude position of the electron density maximum in the ionospheric layer practically coincides with the minimum position of the refractive attenuation of the sounding signal. During radio occultation of the Earth's ionosphere, the wave vector is parallel to the ionization plane of the sporadic E layer. The propagation of radio waves through its central part (maximum of the electron density) then leads to strong defocusing of the rays, while the passage of waves through the layer edges leads to their focusing. Obviously, the vertical resolution (~2.5 km) of the electron density profile (Fig. 3, left, panel c) is insufficient to describe the structure of a thin layer in the ionosphere, since the altitude of the refractive attenuation minimum (~93.7 km) does not coincide with the altitude of the electron density maximum (~92.5 km) and differs from it by ~1.2 km.

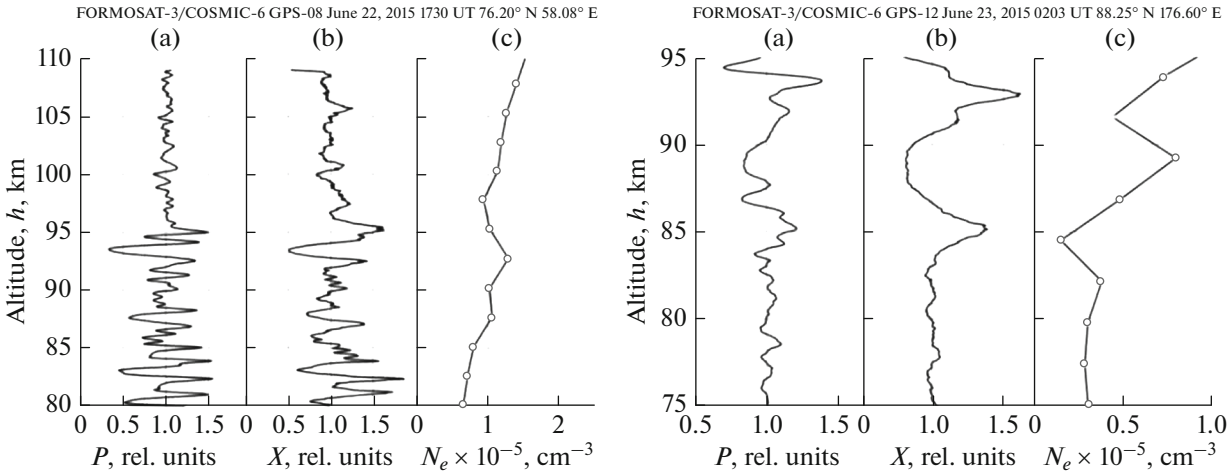

Fig. 3. Altitude profiles of normalized power $P(h)$, refractive attenuation $X(h)$, and electron density $N_e(h)$ obtained from radio occultation data of the FORMOSAT-3/COSMIC-6 satellite in the ionospheric region with coordinates 76.2° N; 58.08° E (left) at 1730 UT on June 22, 2015, and in the region with coordinates 88.25° N; 176.6° E (right) at 0203 UT on June 23, 2015.

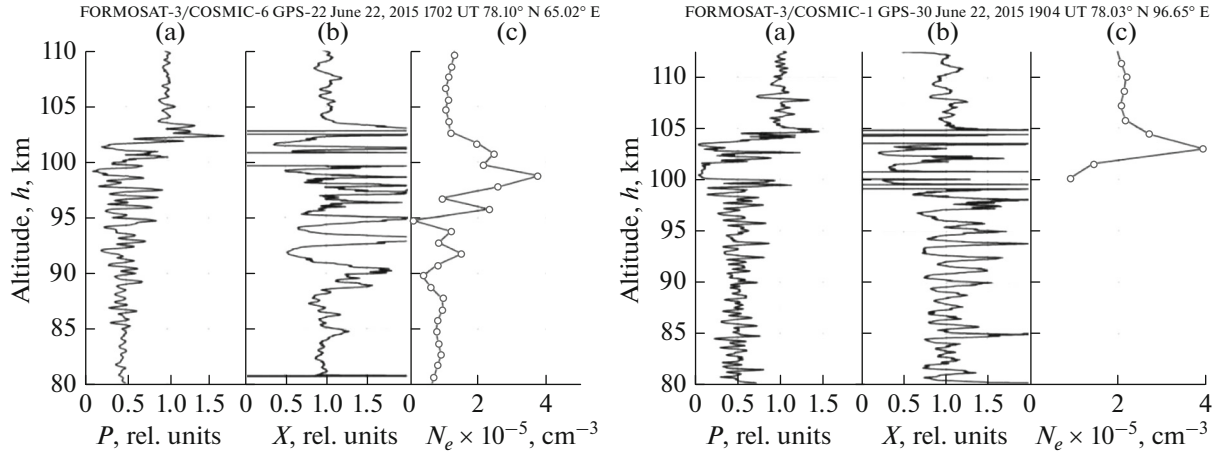

Fig. 4. Altitude profiles of normalized power $P(h)$, refractive attenuation $X(h)$, and electron density $N_e(h)$ obtained from radio occultation measurements of the FORMOSAT-3/COSMIC-6 satellite in the region with coordinates 78.1° N; 65.02° E (left) at 1702 UT on June 22, 2015, and of the FORMOSAT-3/COSMIC-1 satellite in the region with coordinates 78.03°N; 96.65°E (right) at 1914 UT on June 22, 2015.

The other two profiles $P(h)$ and $X(h)$ in Fig. 3 (right, panels a and b), which were obtained from measurements at the boundary between the second and third time intervals, demonstrate very small disturbances on the sounding paths of the ionosphere. This indicates a calm state and the absence of any influence of geomagnetic conditions and X-ray bursts. The S4-index value for variations in power $P(h)$ at altitudes of ~75–95 km (Fig. 3, right, panel a) was found to be less than ~10%. Based on the data in Fig. 3, a layered structure with a vertical size of ~8 km is observed in the Earth's ionosphere at altitudes above 83 km. This isolated ionospheric layer has a typical U-shape, and the altitude of the electron density maximum (~89.0 km) is equal to the altitude of the minimum of the refractive attenuation of radio waves, which confirms the results of previous studies (Gubenko et al., 2018; Gubenko and Kirillovich, 2019, 2020; Pavelyev et al., 2012, 2015).

The vertical profiles $P(h)$ and $X(h)$ in Fig. 4 were obtained from radio occultation measurements performed on June 22 at 1702 UT (left, second interval) and 1914 UT (right, second interval) in the Earth's high-latitude ionosphere. Measurements related to the profiles on the left side of Fig. 4 were performed ~0.5 h after the onset of powerful X-ray bursts and ~1.5 h before the main CME arrived at the planet's magnetosphere. These measurements can be affected by X-ray bursts and are not affected by the geomagnetic conditions of the main phase of the storm. Note that the two sessions of radio occultation measurements presented in Figs. 3 (left) and 4 (left) are practi-

cally coincident in time and space. The separation in time and space between the measurement sessions was small and less than ~30 min and about ~200 km, respectively. Radio waves in the measurement sessions were received by the same low-orbit satellite FORMOSAT-3/COSMIC-6, while the signal transmitters were located on different navigation satellites GPS-08 (Fig. 3) and GPS-22 (Fig. 4). The calculation shows that the sounding paths in the Earth's ionosphere were located rather close to each other in these two sessions. Thus, the divergence angle of the paths at the signal receiving point on the FORMOSAT-3/COSMIC-6 satellite is only ~3.73°, which leads to a path divergence of ~200 km at the planet's limb and ~1900 km near the orbits of the GPS-08 and GPS-22 navigation satellites. Nevertheless, there are dramatic differences in the behavior of the $P(h)$ and $X(h)$ profiles for the measurement sessions considered here. The level of fluctuations at altitudes from ~80 to ~100 km for the $P(h)$ profile in Fig. 4 is significantly higher than that for its analog in Fig. 3. A distinctive feature of sounding of the area with coordinates 78.1° N and 65.02° E is that the average signal power drops to ~0.5 (– 3 dB) at an altitude of ~90 km and remains at the same level with decreasing altitude (Fig. 4). The vertical profiles of the electron density and its maximal values of $\sim 1.3 \times 10^5$ cm^{-3} (Fig. 3, left, panel c) and $\sim 3.9 \times 10^5$ cm^{-3} (Fig. 4, left, panel c) also strongly differ for the indicated measurements.

We suppose that a possible reason for such significant differences is the local nature of the powerful X-ray fluxes during measurements. This can lead to (a) excessive ionization in certain regions of the Earth's ionosphere and the appearance of horizontal gradients, (b) failure to fulfill the condition of local spherical symmetry of the medium during its probing, and (c) multipath and violation of the conditions of geometric optics. An argument in favor of the point (a) is the strong difference in the vertical electron density profiles for the indicated sessions of radio occultation measurements. Violation of the conditions of geometric optics and multipath may be indicated by an obvious discrepancy between the measured power profile $P(h)$ and the refractive attenuation profile $X(h)$ reconstructed with the GO method from the eikonal data (Fig. 4, left, panels a and b).

The measurements related to radio occultation profiles on the right side of Fig. 4, which were performed on June 22 at 1914 UT (second interval), demonstrate strong ionospheric disturbances caused by the effect of both the main phase of the magnetic storm and powerful fluxes of X-ray radiation. As can be seen from the presented data, during radio sounding of this region (78.03° N; 96.65° E) of the Earth's polar cap (ray descends from top to bottom), the power of decimeter radio waves first decreases to ~0.1 (–10 dB) at altitudes from 101.5 to 90.3 km, then increases to ~0.5 (–3 dB), and then remains at the same level as the altitude decreases. Analysis of the two profiles of refractive attenuation $X(h)$ in Fig. 4 (panels b) shows that the average value of X is $\langle X \rangle = 1.0$ (0 dB). This means that there is practically no regular refractive attenuation of radio waves in measurement sessions at altitudes above 50 km. Therefore, we suppose that the attenuation of average signal power $\langle P(h) \rangle$ observed in Fig. 4 may be associated with the absorption of radio waves in the lower ionosphere of the Earth during a geomagnetic storm.

Gorbunov (2017) noted a small atmospheric absorption (up to –1 dB) of radio waves, which can be noticed at GPS frequencies according to the data of radio occultation measurements. The absorption of radio waves in the polar cap caused by solar-wind particles (protons with energies of tens of MeV) and auroral absorption associated with precipitation of electrons with energies of 20–100 keV are a characteristic feature of the Earth's high-latitude ionosphere and are often observed during geomagnetic storms. During the period of solar flares directed towards the Earth, which manifest themselves in the form of a sharp increase in X-ray fluxes, ionospheric disturbances are indicated by an increased level of ionization in the D and E regions (Bryunelli and Namgaladze, 1988).

We reliably detected the absorption of signals in the $L1$ range in two sessions (Fig. 4) of FORMOSAT-3/COSMIC radio occultation measurements in the E and D regions of the Earth's high-latitude ionosphere. In one of them, the integral attenuation of the radio wave power reached –10 dB, and then returned to –3 dB (right, panel a). In another measurement session, it was –3 dB (left, panel a). Using the vertical profiles of the integral signal absorption and solving the inverse problem, one can determine the altitude profiles of the absorption coefficient (Z) of radio waves and can estimate the effective collision number (ν) of an electron per unit time in the Earth's lower ionosphere (Kolosov et al., 1969).

The absorption of radio waves in the Earth's ionosphere is caused by collisions of electrons with ions and neutral molecules. For this reason, part of the energy imparted by the electromagnetic field to the electrons is spent on an increase in the energy of the chaotic motion of plasma particles and leads to its heating. At each impact, the electron on average transfers to the ion or molecule the momentum $m\mathrm{d}\mathbf{r}/\mathrm{d}t$, where $\mathrm{d}\mathbf{r}/\mathrm{d}t$ is the ordered velocity of the electrons under the action of the field. If ν is the effective collision number of an electron per second, then its momentum per unit time changes by the $m\nu\,\mathrm{d}\mathbf{r}/\mathrm{d}t$ value. The change in the momentum of an electron due to collisions is equivalent to the action of a certain frictional force.

Assuming that the radio wave frequency of $\omega = 2\pi f$ satisfies the inequality $\omega^2 \gg \nu^2$, the following estimate of absorption coefficient Z of radio waves was obtained by Kolosov et al. (1969):

$$Z = \frac{e^2 N_e \nu}{\pi m c f^2} = 2.70 \times 10^{-3} \frac{N_e \nu}{f^2}, \quad [Z] = \text{cm}^{-1}, \qquad (2)$$

where m is the electron mass, e is the electron charge, and c is the speed of light. N_e is expressed in cm^{-3}, ν is in s^{-1}, and f is in Hz. If the flux of radio waves during their propagation through the ionosphere experiences absorption, then the normalized power P of the signal at the receiving point will be equal to (Kolosov et al., 1969):

$$P = \exp\left[-\int_{h_{min}}^{h_{max}} Z\, ds\right] = \exp\left[\frac{-2.70 \times 10^{-3}}{f^2} \int_{h_{min}}^{h_{max}} N_e \nu ds\right]. \qquad (3)$$

In this expression, integration from h_{min} to h_{max} is performed along the path of the probing radio ray. As can be seen from formula (2), to estimate the ν parameter, it is necessary to know the vertical profile of the absorption coefficient and the electron density distribution over the altitude. The solution of the inverse problem of the signal-power absorption with expression (3) allows the determination of the vertical profile of the absorption coefficient of radio waves $Z(h)$. Next, it is easy to find the vertical profile of the ν parameter in the Earth's lower ionosphere using formula (2) with the available $N_e(h)$ profiles (Fig. 4, panels c) and the $Z(h)$ dependences obtained from the solution of the inverse problem.

3. CONCLUSIONS

Approximately 100 sessions of FORMOSAT-3/COSMIC radio occultation measurements during the magnetic storm on June 22–23, 2015 in the Earth's high-latitude ionosphere were processed and analyzed. Ionospheric disturbances in the characteristics of radio waves are shown to be caused by both geomagnetic conditions and the activity of powerful X-ray flares during the measurements. The sessions of radio occultation measurements performed after the beginning (1630 UT on June 22) of powerful bursts of X-ray radiation or during the main phase of a geomagnetic storm are characterized by increased levels of ionization in the D and E regions of the planet's ionosphere. Here, the maximal values of the electron density exceed $\sim 1.3 \times 10^5\ \text{cm}^{-3}$ and can reach values of $\sim 3.9 \times 10^5\ \text{cm}^{-3}$ (Figs. 3 and 4).

A search for the absorption of decimeter radio waves (wavelength of ~19 cm) at a GPS carrier frequency of $f_1 = 1545.42$ MHz was carried out. According to the results of the FORMOSAT-3/COSMIC data analysis, the absorption of decimeter radio waves in the D and E regions of the Earth's high-latitude ionosphere was detected for the first time. It was found that the absolute value of the integral absorption on the radio occultation sounding paths is ~3 dB in an altitude range of ~50–90 km and, in some cases, reaches ~10 dB at altitudes of ~90–95 km. The practical significance of the study of the absorption effects of radio waves in the ionospheric D and E regions is associated with ensuring the uninterrupted operation of space radio communication and navigation systems.

FUNDING

This work was carried out within the framework of a state assignment and partially supported by the Russian Foundation for Basic Research, project no. 19-02-00083 A.

REFERENCES

Astafyeva, E., Zakharenkova, I., and Alken, P., Prompt penetration electric fields and the extreme topside ionospheric response to the 22–23 June 2015 geomagnetic storm as seen by the Swarm constellation, *Earth Planets Space*, 2016, vol. 68, id 152. https://doi.org/10.1186/s40623-016-0526-x

Astafyeva, E., Zakharenkova, I., Huba, J.D., Doornbos, E., and Ijssel, J., Ionospheric and thermospheric effects of the June 2015 geomagnetic disturbances: Multi-instrumental observations and modeling, *J. Geophys. Res.*, 2017, vol. 122, pp. 1–27. https://doi.org/10.1002/2017JA024174

Baker, D.N., Jaynes, A.N., Turner, D.L., et al., A telescopic and microscopic examination of acceleration in the June 2015 geomagnetic storm: Magnetospheric Multiscale and Van Allen Probes study of substorm particle injection, *Geophys. Res. Lett.*, 2016, vol. 43, pp. 6051–6059. https://doi.org/10.1002/2016GL069643

Bryunelli, B.E. and Namgaladze, A.A., *Fizika ionosfery* (Physics of the Ionosphere), Moscow: Nauka, 1988.

Gorbunov, M.E., Radio occultation of the atmosphere, in *Dinamika volnovykh i obmennykh protsessov v atmosfere* (Dynamics of Wave and Exchange Processes in the Atmosphere), Moscow: GEOS, 2017, ch. 4, pp. 407–457.

Gubenko, V.N. and Kirillovich, I.A., Modulation of sporadic E layers by small-scale atmospheric waves in Earth's high-latitude ionosphere, *Sol.-Terr. Phys.*, 2019, vol. 5, pp. 98–108. https://doi.org/10.12737/stp-53201912

Gubenko, V.N. and Kirillovich, I.A., Association of inclined sporadic E-layers and small-scale atmospheric waves in Earth's ionosphere, *Cosmic Res.*, 2020, vol. 58, pp. 139–149. https://doi.org/10.1134/S0010952520030028

Gubenko, V.N., Pavelyev, A.G., Kirillovich, I.A., and Liou, Y.-A., Case study of inclined sporadic e layers in the Earth's ionosphere observed by CHAMP/GPS radio occultations: coupling between the tilted plasma layers and internal waves, *Adv. Space Res.*, 2018, vol. 61, pp. 1702–1716. https://doi.org/10.1016/j.asr.2017.10.001

Hocke, K., Oscillations of global mean TEC, *J. Geophys. Res.*, 2008, vol. 113, A04302. https://doi.org/10.1029/2007JA012798

Kolosov, M.A., Armand, N.A., and Yakovlev, O.I., *Rasprostranenie radiovoln pri kosmicheskoi svyazi* (Radio-

wave Propagation in Space Communication), Moscow: Svyaz', 1969.

Liou, Y.-A., Pavelyev, A.G., Liu, S.-F., Pavelyev, A.A., Yen, N., Huang, C.-Y., and Fong, C.-J., FORMOSAT-3/COSMIC GPS radio occultation mission: Preliminary results, *IEEE Trans. Geosci. Remote Sens.*, 2007, vol. 45, pp. 3813–3826.

Mansilla, G.A., Ionospheric response to the magnetic storm of 22 June 2015, *Pure Appl. Geophys.*, 2018, vol. 175, pp. 1139–1153. https://doi.org/10.1007/s00024-017-1741-5

Pavelyev, A.G., Liou, Y.A., Wickert, J., Gubenko, V.N., Pavelyev, A.A., and Matyugov, S.S., New applications and advances of the GPS radio occultation technology as recovered by analysis of the FORMOSAT-3/COSMIC and CHAMP data-base, in *New Horizons in Occultation Research: Studies in Atmosphere and Climate*, Steiner, A., Pirscher, B., Foelsche, U., and Kirchengast, G., Eds., Berlin: Springer, 2009, pp. 165–178. https://doi.org/10.1007/978-3-642-00321_9.

Pavelyev, A.G., Liou, Y.-A., Zhang, K., Wang, C.S., Wickert, J., Schmidt, T., Gubenko, V.N., Pavelyev, A.A., and Kuleshov, Y., Identification and localization of layers in the ionosphere using the eikonal and amplitude of radio occultation signals, *Atmos. Meas. Tech.*, 2012, vol. 5, pp. 1–16. https://doi.org/10.5194/amt-5-1-2012

Pavelyev, A.G., Liou, Y.-A., Matyugov, S.S., Pavelyev, A.A., Gubenko, V.N., Zhang, K., and Kuleshov, Y., Application of the locality principle to radio occultation studies of the Earth's atmosphere and ionosphere, *Atmos. Meas. Tech.*, 2015, vol. 8, pp. 2885–2899. https://doi.org/10.5194/amt-8-2885-2015

Reiff, P.H., Daou, A.G., Sazykin, S.Y., et al., Multispacecraft observations and modeling of the 22/23 June 2015 geomagnetic storm, *Geophys. Res. Lett.*, 2016, vol. 43, pp. 7311–7318. https://doi.org/10.1002/2016GL069154

Wickert, J., Pavelyev, A.G., Liou, Y.A., Schmidt, T., Reigber, C., Igarashi, K., Pavelyev, A.A., and Matyugov, S., Amplitude scintillations in GPS signals as a possible indicator of ionospheric structures, *Geophys. Res. Lett.*, 2004, vol. 31, L24801. https://doi.org/10.1029/2004GL020607

Yakovlev, O.I., Pavelyev, A.G., and Matyugov, S.S., *Sputnikovyi monitoring Zemli: Radiozatmennyi monitoring atmosfery i ionosfery* (Satellite Monitoring of the Earth. Radio Occultation Monitoring of the Atmosphere and Ionosphere), Moscow: Librokom, 2014.

Yakovlev, O.I., Matugov, S.S., and Pavelyev, A.A., Results of studying the daytime polar ionosphere by the radio occultation method on satellite-to-satellite paths, *Radiophys. Quantum Electron.*, 2019, vol. 62, pp. 174–182. https://doi.org/10.1007/s11141-019-09965-y

Yasyukevich, Y., Vasilyev, R., Ratovsky, K., Setov, A., Globa, M., Syrovatskii, S., Yasyukevich, A., Kiselev, A., and Vesnin, A., Small-scale ionospheric irregularities of auroral origin at mid-latitudes during the 22 June 2015 magnetic storm and their effect on GPS positioning, *Remote Sens.*, 2020, vol. 12, id 1579. https://doi.org/10.3390/rs12101579

Zeng, Z. and Sokolovskiy, S., Effect of sporadic E cloud on GPS radio occultation signal, *Geophys. Res. Lett.*, 2010, vol. 37, L18817. https://doi.org/10.1029/2010GL044561

Translated by A. Ivanov